



Cite this: DOI: 10.1039/d5cc03674g

Received 30th June 2025,  
Accepted 7th September 2025

DOI: 10.1039/d5cc03674g

rsc.li/chemcomm

# Continuous ethanol monitoring in skin gas using a screen-printed biosensor

Isao Shitanda,<sup>a</sup> Hayato Jibiki,<sup>a</sup> Noya Loew,<sup>\*a</sup> Hikari Watanabe<sup>a</sup> and Masayuki Itagaki<sup>ab</sup>

Herein, we report an enzyme-based electrochemical biosensor composed of screen-printed electrodes on a polyimide film for detecting ethanol in skin gas. The linear range and sensitivity were 50 to 150 ppb and 344 mA cm<sup>-2</sup> ppb<sup>-1</sup>, respectively. On-body testing showed that skin gas ethanol increased from 1500 s onwards after alcohol consumption.

Monitoring ethanol concentrations in human blood is crucial for assessing alcohol consumption, disease diagnosis, and forensic medicine.<sup>1,2</sup> Ingested ethanol is absorbed in the gastrointestinal tract, passes through blood vessels, and is partially discharged as exhaled breath or skin gas.<sup>3,4</sup> Therefore, accurate detection of ethanol concentrations in exhaled breath or skin gas can be used to predict blood alcohol levels and measure the degree of intoxication. However, the concentration of skin gas components emitted from humans is at the ppb level, which is very low compared to the concentration of components in exhaled breath.<sup>3,5,6</sup> For example, the ethanol concentration in exhaled breath ranges from 37–207 ppb, whereas in skin gas, it is in the range of 3.6–79.2 ppb min<sup>-1</sup>.<sup>3</sup> Therefore, highly sensitive sensors are needed for skin gas measurements.

However, unlike exhaled breath sampling, skin gas sampling may require less conscious involvement from the person being tested. Therefore, skin gas sensors are envisioned as effective and simple tools for the screening of diseases and metabolic activity without limiting the behavior of the tested person.<sup>5,7</sup> In contrast to exhaled breath measurements, skin gas measurements have the potential for continuous monitoring.

Recently, we reported the successful fabrication of a screen-printed biosensor for detecting acetaldehyde gas, suitable for measuring skin gas concentration levels.<sup>8</sup> The sensor was fabricated by screen-printing a mesoporous carbon working

electrode, carbon counter electrode, and Ag/AgCl reference electrode onto a porous polyimide film. MgO-templated carbon (MgOC), which features controlled pore sizes, has been frequently employed as the working electrode in biosensors and biofuel cells.<sup>9–11</sup> To firmly bind the enzyme to the MgOC surface, MgOC was grafted with glycidyl methacrylate (GMA) to form grafted MgOC (GMgOC).<sup>12</sup>

Furthermore, a polydimethylsiloxane (PDMS) chamber was attached to the acetaldehyde electrode and filled with a measurement solution containing the electrolyte and mediator.<sup>8</sup> The sample gas was delivered to the electrode through the porous polyimide film. This led to the accumulation of acetaldehyde in the mesoporous GMgOC, thereby increasing the sensitivity of the sensor. The sensor had a dynamic range of 0.02 to 0.1 ppm, which was low enough for skin gas measurements.<sup>8</sup> In this study, we fabricated an ethanol sensor in a similar manner and utilized it for the continuous monitoring of ethanol in skin gas during on-body tests.

Electrodes were screen-printed on the porous polyimide film (PIM-1000N; Tokyo Ohka Kogyo Co.) as previously reported.<sup>8</sup> The printed sensor was modified by drop-casting 10 µL nicotinamide adenine dinucleotide (NAD)-dependent alcohol dehydrogenase (ADH; Fujifilm Wako Pure Chemicals) solution (20 U) in 100 mM phosphate buffer, pH 8.0, followed by drying under reduced pressure (0.1 MPa) for 1.5 h. Before the measurements, agarose gel was fabricated by dissolving agarose (Nippon Gene Co.) in 100 mM phosphate buffer (pH 8.0) by heating and stirring. The dissolved gel was allowed to cool before methoxy-5-methylphenazine methyl sulfate (1-MeO PMS; Fujifilm Wako Pure Chemicals) and NAD was added and was stirred. Finally, the gel solution (0.5 mL) was drop-cast onto the electrodes and allowed to solidify at room temperature. The measurements were immediately performed.

The gas delivery system used in this study was similar to that used previously,<sup>8</sup> with a mass flow controller added before the measurement cell to control the sample gas flow rate. Ethanol gas was measured using chronoamperometry, where a potential of −0.01 V was applied for 60 s, followed by a potential of 0.4 V using a potentiostat (PalmSens).

<sup>a</sup> Department of Pure and Applied Chemistry, Faculty of Science and Technology, Tokyo University of Science, 2641 Yamazaki, Noda, Chiba 278-8510, Japan.  
E-mail: shitanda@rs.tus.ac.jp, noya-loew@rs.tus.ac.jp

<sup>b</sup> Research Institute for Science and Technology, Tokyo University of Science, 2641 Yamazaki, Noda, Chiba 278-8510, Japan



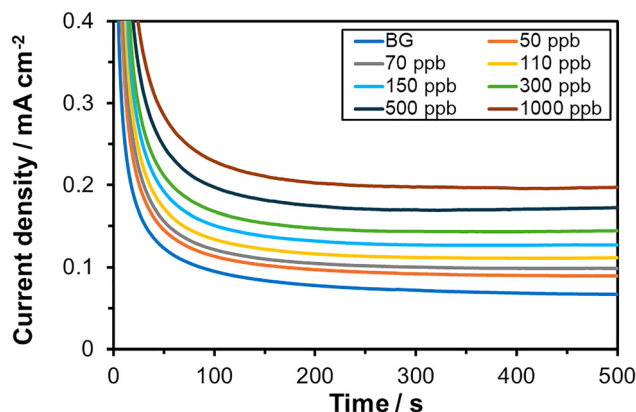


Fig. 1 Representative chronoamperograms of the ethanol gas biosensor. Measurement conditions: 100 mM 1-MeO PMS, 5 mM NAD, 0.1 M phosphate buffer, pH 8.0, in agarose; 0.4 V vs. Ag/AgCl; gas flow rate: 0.37 L min<sup>-1</sup>.

The fabricated ethanol gas sensor was characterized by chronoamperometry (Fig. 1). A Michaelis–Menten-type dependency on the ethanol concentration in the sample gas was observed, with an apparent  $K_m$  value of 277 ppb and a maximum current density of 0.13 mA cm<sup>-2</sup> (Fig. 2). Furthermore, a linear range of 50–150 ppb was observed with a sensitivity of 344 mA cm<sup>-2</sup> ppb<sup>-1</sup> (Fig. 2, inset). The dynamic range was then extended to 1 ppm (Fig. 2). While optical sensors can measure ethanol gas concentrations in the low ppb range,<sup>3,13</sup> electrochemical sensors in the literature measure concentrations in the hundreds of ppb to ppm range.<sup>14–16</sup> Therefore, the ethanol gas sensor developed in this study is unusually sensitive for an electrochemical sensor. Additionally, because the concentration of ethanol in the human skin gas emitted during alcohol consumption ranges from 70 to 110 ppb,<sup>3</sup> these results indicate that the developed ethanol gas biosensor is suitable for monitoring skin gas.

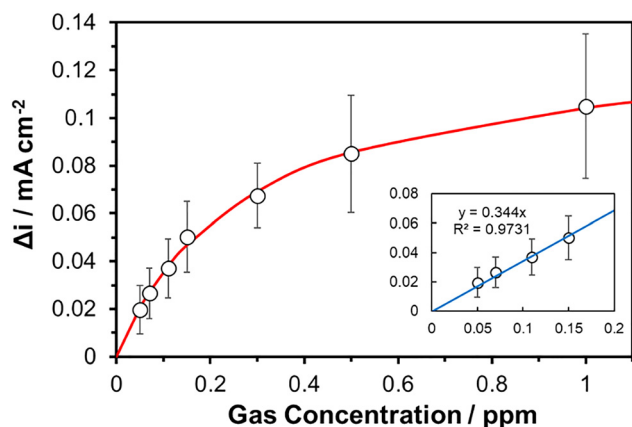


Fig. 2 Concentration dependency of the ethanol gas biosensor. Measurement conditions: 100 mM 1-MeO PMS; 5 mM NAD; 0.1 M phosphate buffer; pH 8.0; in agarose; 0.4 V vs. Ag/AgCl; gas flow rate: 0.37 L min<sup>-1</sup>.  $N = 3$ , 90% confidence interval. Red line indicates a Michaelis–Menten-type fit. Inset: close-up of the linear range with a linear regression line.

Furthermore, the agarose gel electrolyte allowed the sensor to be more flexible compared to the liquid electrolyte filled-PDMS chamber used previously.<sup>8</sup> With the gel electrolyte, there was also less risk of the measurement solution leaking and coming in contact with the skin. Although the components of the measurement solution are not harmful, contact with the skin should be avoided.

For proof-of-concept purposes, one of the authors conducted a self-test ( $N = 1$ ) by consuming different alcoholic beverages and monitoring the sensor response. This procedure was conducted only to validate the technical operation of the device and does not constitute a clinical or human subject study. For this on-body self-test, a sensor was attached to the wrist of the author (male, 40s) using surgical tape and connected to a potentiostat (Fig. 3). The wrist was chosen as the measurement site because of its abundant blood vessels, thin skin, and low risk of interference from perspiration. Ethanol in blood diffuses into the interstitial fluid through the skin and is emitted as skin gas. The skin gas passes through the porous polyimide of the sensor device and reaches the working electrode, where the ethanol is detected.

After measuring the baseline response for 10 min, the author consumed beverages containing varying percentages of alcohol (Fig. 4). The start of beverage intake was set to 0 s. The alcoholic beverages consumed were 500 mL containing 5% alcohol, 350 mL containing 9% alcohol, 175 mL containing 7% alcohol (twice),

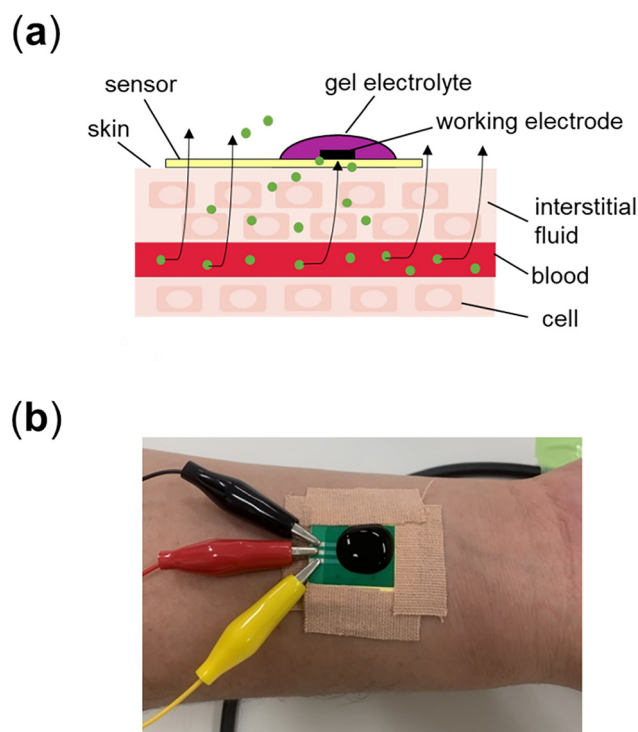


Fig. 3 On-body test of the ethanol gas biosensor. (a) Scheme of the measurement principle with the sensor device on the skin. Green dots represent ethanol molecules. Arrows represent movement of ethanol molecules. (b) Photograph of the sensor device attached to the wrist of the test subject.



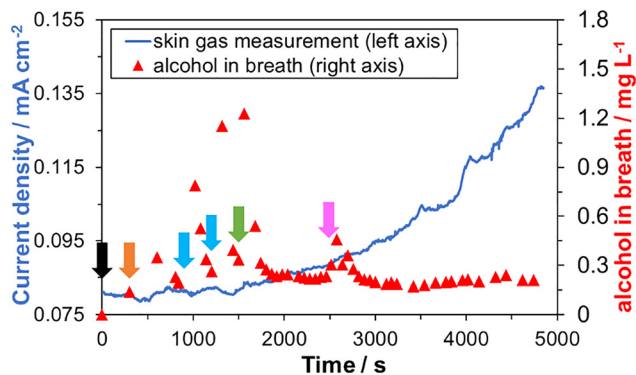


Fig. 4 Results of the on-body test of the ethanol gas biosensor. (blue line) Response current of the ethanol gas biosensor. (red triangles) Alcohol concentration in breath according to a commercial alcohol detector. (arrows) Intake of alcoholic beverage: (black arrow) 500 mL 5% alcohol; (orange arrow) 350 mL 9% alcohol; (blue arrows) 175 mL 7% alcohol; (green arrow) 20 mL 40% alcohol; and (pink arrow) 100 mL 3% alcohol.

20 mL containing 40% alcohol, and 100 mL containing 3% alcohol. Simultaneously, the alcohol concentration in the breath of the author was measured at 1 min intervals using a commercially available alcohol detector (AC-018, Toyo Mark Manufacturing Co., Ltd).

The response of the skin gas sensor remained at the baseline for 1500 s and then increased significantly for the remaining measurements (Fig. 4). In contrast, the alcohol concentration in the breath spiked after every intake of alcohol and then remained constant (Fig. 4). This discrepancy can be explained by the differences in the processes through which ethanol is present in the breath and skin gas. Directly after alcohol consumption, residual ethanol in the mouth and throat increases the concentration of ethanol in the breath, leading to the observed spikes in breath measurements (Fig. 4). The consumed alcohol is then absorbed into the bloodstream. A fraction of the ethanol in the blood diffuses into the alveoli of the lungs and is expelled *via* breath. Another fraction of ethanol in the blood diffuses into the interstitial fluid and is expelled as skin gas. In contrast to the skin, the lungs are optimized for gas exchange. Therefore, it is reasonable to assume that ethanol emissions through the skin are less efficient and may have a larger time lag. Most ethanol is metabolized in the liver and removed from the bloodstream. These processes lead to a time lag between alcohol consumption and reliable detection of ethanol in breath and skin gases. This delayed detection of ethanol in the breath was not observed in this study, as the ethanol concentration in the breath was dominated by the contribution of residual ethanol in the mouth and throat (Fig. 4). The ethanol concentration in the skin gas was not affected by the residuals, and an increasing ethanol concentration was detected from 1500 s onwards (Fig. 4).

The response current density difference from the baseline at the end of the on-body test was approximately  $0.057 \text{ mA cm}^{-2}$ , which is slightly higher than the linear range of the skin gas sensor (Fig. 4). Using the sensitivity of the linear range,

the observed response corresponded to 166 ppb; as calculated from the Michaelis–Menten-type fit of the calibration to 207 ppb of ethanol in skin gas. In both cases, the observed value was higher than the range reported by Arakawa *et al.* for ethanol in skin gas after alcohol consumption (70–110 ppb<sup>3</sup>). However, Arakawa *et al.* monitored the occurrence of ethanol in skin gas after a single alcohol intake, whereas we monitored the ethanol in skin gas during and after several consecutive alcohol intakes. Furthermore, the ethanol concentration in breath reported by Arakawa *et al.* was about  $0.13 \text{ mg L}^{-1}$ ,<sup>3</sup> while the ethanol concentration in breath at the end of this study was significantly higher at  $0.21 \text{ mg L}^{-1}$  (Fig. 4), corroborating with the observed higher ethanol concentration.

In this study, a skin gas sensor for ethanol monitoring was successfully developed and tested using an on-body test. The electrodes of the sensor, including the porous carbon working electrode, were screen printed onto a porous polyimide film. The ethanol gas reached the enzyme-modified sensing electrode through the porous polyimide film. A gel electrolyte was used to improve flexibility and safety during the on-body tests. In laboratory tests, the sensor exhibited a linear range of 50–150 ppb and a dynamic range of up to 1 ppm. The sensitivity in the linear range was  $344 \text{ mA cm}^{-2} \text{ ppb}^{-1}$ . A clear increase in skin gas ethanol was observed during an on-body test 1500 s after the start of alcohol consumption. An ethanol concentration of 166–207 ppb was detected at the end of the on-body test approximately 80 min after the beginning of alcohol consumption. Therefore, the electrochemical skin gas sensor can be used to easily monitor ethanol in the skin gas.

I. S. conceptualized the work. H. J. carried out the experiments. H. J. and N. L. wrote the initial version of the manuscript. I. S. and N. L. revised and finalized the manuscript. I. S., H. W., and M. I. supervised the work.

This research was supported by a Grant-in-Aid for Scientific Research (KAKENHI B) and the President's Priority Research Program of Tokyo University of Science.

## Conflicts of interest

There are no conflicts to declare.

## Data availability

All data supporting the findings of this study are included within the article. The data supporting this study are available from the corresponding author upon reasonable request.

## Notes and references

- W. Jones, F. C. Kugelberg, A. Holmgren and J. Ahlner, *Forensic Sci. Int.*, 2008, **181**, 40–46, DOI: [10.1016/j.forsciint.2008.08.010](https://doi.org/10.1016/j.forsciint.2008.08.010).
- M. J. Lewis, *J. Forensic Sci. Soc.*, 1986, **26**, 95–113, DOI: [10.1016/S0015-7368\(86\)72453-5](https://doi.org/10.1016/S0015-7368(86)72453-5).
- T. Arakawa, T. Aota, K. Iitani, K. Toma, Y. Iwasaki and K. Mitsubayashi, *Talanta*, 2020, **219**, 121187, DOI: [10.1016/j.talanta.2020.121187](https://doi.org/10.1016/j.talanta.2020.121187).
- K. Naitoh, T. Tsuda, K. Nose, T. Kondo, A. Takasu and T. Hirabayashi, *Instrum. Sci. Technol.*, 2002, **30**, 267–280, DOI: [10.1081/Ci-120013506](https://doi.org/10.1081/Ci-120013506).



- 5 P. Mochalski, J. King, K. Unterkofler, H. Hinterhuber and A. Amann, *J. Chromatogr. B: Anal. Technol. Biomed. Life Sci.*, 2014, **959**, 62–70, DOI: [10.1016/j.jchromb.2014.04.006](#).
- 6 J. C. Anderson, A. L. Babb and M. P. Hlastala, *Ann. Biomed. Eng.*, 2003, **31**, 1402–1422, DOI: [10.1114/1.1630600](#).
- 7 Y. Sekine, S. Toyooka and S. F. Watts, *J. Chromatogr. B: Anal. Technol. Biomed. Life Sci.*, 2007, **859**, 201–207, DOI: [10.1016/j.jchromb.2007.09.033](#).
- 8 I. Shitanda, T. Oshimoto, N. Loew, M. Motosuke, H. Watanabe, T. Mikawa and M. Itagaki, *Biosens. Bioelectron.*, 2023, **238**, 115555, DOI: [10.1016/j.bios.2023.115555](#).
- 9 H. Funabashi, K. Murata and S. Tsujimura, *Electrochemistry*, 2015, **83**, 372–375, DOI: [10.5796/electrochemistry.83.372](#).
- 10 H. Funabashi, S. Takeuchi and S. Tsujimura, *Sci. Rep.*, 2017, **7**, 45147, DOI: [10.1038/srep45147](#).
- 11 S. Tsujimura, K. Murata and W. Akatsuka, *J. Am. Chem. Soc.*, 2014, **136**, 14432–14437, DOI: [10.1021/ja5053736](#).
- 12 I. Shitanda, T. Kato, R. Suzuki, T. Aikawa, Y. Hoshi, M. Itagaki and S. Tsujimura, *Bull. Chem. Soc. Jpn.*, 2020, **93**, 32–36, DOI: [10.1246/bcsj.20190212](#).
- 13 K. Iitani, K. Toma, T. Arakawa and K. Mitsubayashi, *Anal. Chem.*, 2019, **91**, 9458–9465, DOI: [10.1021/acs.analchem.8b05840](#).
- 14 K. Mitsubayashi, K. Yokoyama, T. Takeuchi and I. Karube, *Anal. Chem.*, 1994, **66**, 3297–3302, DOI: [10.1021/ac00092a004](#).
- 15 T. R. L. C. Paixão and M. Bertotti, *J. Electroanal. Chem.*, 2004, **571**, 101–109, DOI: [10.1016/j.jelechem.2004.04.015](#).
- 16 K. Mitsubayashi, H. Matsunaga, G. Nishio, S. Toda and Y. Nakanishi, *Biosens. Bioelectron.*, 2005, **20**, 1573–1579, DOI: [10.1016/j.bios.2004.08.007](#).

